Acta Oceanol. Sin., 2023, Vol. 42, No. 6, P. 78–88
https://doi.org/10.1007/s13131-022-2109-y
http://www.aosocean.com
E-mail: ocean2@hyxb.org.cn

Obtaining accurate measurements of the sea surface height from a GPS buoy

Wanlin Zhai[1], Jianhua Zhu[1], Chuntao Chen[2*], Wu Zhou[3], Longhao Yan[1], Yufei Zhang[3], Xiaoqi Huang[1], Kai Guo[1]

[1] National Ocean Technology Center, Tianjin 300112, China

[2] School of Ocean, Yantai University, Yantai 266004, China

[3] National Satellite Ocean Application Service, Beijing 100081, China

Received 26 April 2022; accepted 27 September 2022

Abstract

A dedicated GPS buoy is designed for calibration and validation (Cal/Val) of satellite altimeters since 2014. In order to evaluate the accuracy of the sea surface height (SSH) measured by the GPS buoy, twelve campaigns have been done within China sea area between 2014 and 2021. In six of these campaigns, two static Global Navigation Satellite System stations were installed at distances of <1 km and 19 km from the buoy to assess how the baseline length influenced the derived SSH from the buoy solutions. The GPS buoy data was processed using the GAMIT/GLOBK software+TRACK module and CSRS-PPP tool to achieve the SSH. The SSH was compared with conventionally tide gauge (TG) data to evaluate the accuracy of the buoy with the standard deviation of the height element. The results showed that the difference in the standard deviation of the SSH from the buoy and the TG was less than 16 mm. The SSHs processed with different ephemeris (Ultra-Rapid, Rapid, Final) were not significantly different. When the baseline length was 19 km, the SSH solution of the GPS buoy performed well, with standard bias of less than 26 mm between the heights measured by the buoy and TG, meaning that the buoy could be used for Cal/Val of altimeters. The bias between the Canadian Spatial Reference System-precise point positioning tool and the TRACK varied a lot, and some of them were over 130 mm. This deemed too high to be useful for Cal/Val of satellite altimeters. Moreover, the GPS buoy solutions processed by GAMIT/GLOBK software+TRACK module were used for in-orbit Cal/Val of HY-2B/C satellites in ten campaigns. The SSH and significant wave height of the altimeters showed good agreements with the GPS buoy solutions.

Key words: GPS buoy, sea surface height, baseline length, precise point positioning, satellite altimeter, HY-2

Citation: Zhai Wanlin, Zhu Jianhua, Chen Chuntao, Zhou Wu, Yan Longhao, Zhang Yufei, Huang Xiaoqi, Guo Kai. 2023. Obtaining accurate measurements of the sea surface height from a GPS buoy. Acta Oceanologica Sinica, 42(6): 78–88, doi: 10.1007/s13131-022-2109-y

1 Introduction

GPS buoy has been used for calibration and validation (Cal/Val) of satellite altimeters since the Topex/POSEIDON which was launched in 1992. Scientists have developed many kinds of GPS buoys to collect sea surface height (SSH) data that support the Cal/Val of satellite altimeters (Ménard et al., 1994; Watson, 2005; Chen et al., 2019; Zhou et al., 2020). The Cal/Val results using the GPS buoy do not need ocean geophysical correction such as ocean tide, mean sea level, inverse barometer , etc., and can achieve the most accurate SSH biases (Babu et al., 2015; Ardalan et al., 2018; Chen et al., 2019). The satellite altimeter has an accuracy of 20–40 mm in the measurement of SSH (Fu et al., 1994), so *in-situ* measurements by a GPS buoy should have the same accuracy or higher. The bias of the altimeters was determined using the dedicated GPS buoys over the last few decades (Bonnefond et al., 2013; Ardalan et al., 2018; Zhou et al., 2020). Dedicated GPS buoys have also been used to determine the datum of coastal tide gauges (TG) (Watson et al., 2008), support tsunami research (Kato et al., 2010), and monitor the water surface elevation (Salleh and Daud, 2015; Lin et al., 2017), etc.

To calibrate an altimeter using a GPS buoy, at least one static GPS station should be placed to determine the datum of the GPS buoys (Watson et al., 2008; Ardalan et al., 2018). The GPS buoy should be as close to the static station as possible to ensure the accuracy of the kinematic solutions. However, when the altimeters fly over from land to ocean or from ocean to land, the waveforms are usually distorted, and the SSH of the altimeter is not accurate. Therefore, the GPS buoy was usually moored 15–30 km from land/island in Cal/Val campaigns. The baseline length from the buoy to the static GPS station, which may affect the accuracy of SSH derived from the GPS buoy (Dong et al., 2002; Watson, 2005; Martinez-Benjamin et al., 2004; Zhai et al., 2019). At present, the static and kinematic Global Navigation Satellite System (GNSS) data were usually processed together to get the accurate SSH using the GAMIT/GLOBK software and TRACK module (Watson et al., 2008; Herring et al., 2018; Zhai et al., 2019; Zhou et al., 2020). Studies have shown that a GPS buoy can measure the SSH with an accuracy of less than 40 mm in a baseline length of ~30 km from the static GPS station (Zhai et al., 2019; Chen et al., 2019).

There is another GPS data processing technology called precise point positioning (PPP), which is not affected by the static stations in producing the SSH. It was first developed by Zumberge et al. (1997), and the accuracy of this technology has continuously improved over time. Crétaux et al. (2018) used this technology (GINS software developed by CNES) to calibrate the

*Corresponding author, E-mail: chenchuntao@ytu.edu.cn

Envisat radar altimeter over Lake Issykkul. The Canadian Spatial Reference System (CSRS) has developed the CSRS-PPP online tool that provides positioning data with centimeter-level accuracies. In this study, we used the CSRS-PPP tool to achieve the SSH and compared with the data from the GPS buoy and TG.

In order to calibrate the HY-2 altimeters in the China sea area, a dedicated GPS buoy has been developed by the National Ocean Technology Center (NOTC) (Chen et al., 2019, 2021; Zhai et al., 2019). To evaluate the accuracy of the SSH measurements from the buoy, twelve campaigns have been done in China sea area between 2014 and 2021. The campaigns are described together with the GPS buoy and the quality of the buoy data in Section 2. Then, the quality of the SSH data from the GPS buoy collected over short periods is compared with conventionally collected data from a TG installed nearby. Also, in six of the twelve campaigns, two static GPS stations are set up at baseline lengths of <1 km and 19 km, respectively. The accuracy of the CSRS-PPP tool is also evaluated in Section 3. The on-orbit Cal/Val results of HY-2B/C are described and analyzed in Section 4. Finally, conclusion and discussion are provided in Section 5.

2 Methods

2.1 *Introduction of the tests*

The GPS buoy that we tested in this study was initially designed and manufactured by the NOTC for Cal/Val of the HY-2A altimeters (Chen et al., 2019; Zhai et al., 2019). The buoy is comprised by three compressed cell polystyrene floats and a capsule that are held together with three stainless sticks (Fig. 1). The shape of the buoy was designed to minimize the influence of waves and the results so far have shown that it is very stable at sea states of 4 on the Beaufort scale. A choke ring antenna (Trimble 59900) and a dual-frequency GPS receiver (Trimble Net R9) were placed on the top and the capsule of the buoy, respectively. This shields any GPS signals reflected by the water and minimizes the influence of multipath, meaning that the measurements are more accurate. The antenna phase center has an accuracy of less than 2 mm, according to the National Geodetic Survey's Antenna Calibration Program (https://www.ngs.noaa.gov/ANTCAL/). The height of the GPS antenna reference point above the waterline is strictly measured in the laboratory so that the GPS solutions relate to water surface on which the buoy or the vessel is deployed (Chen et al., 2014). There are also two lithium iron batteries in the lower part of the buoy capsule for power supply and lower the mass center of the buoy to ensure the stability of the GPS buoy in the water.

Twelve campaigns were conducted from 2014 to 2021 in seven places, namely Qinglan (QLAN), Sanya (SY) and Yinggehai (YGH) in Hainan Province, Dongji Island (DJ) in Zhejiang Province, and Dangan (DG1/2), Wailingding (WLD1/2), and Zhiwan (ZW1/2/3/4) islands in Guangdong Province (Table 1 and Fig. 2). Every campaign involved at least one static GPS station and two TGs placed on the wharf. The GPS buoy was moored less than 0.5 km from the wharf and was generally <1 km from the static GPS station in all the campaigns (Fig. 3). At WLD1/2 and ZW1/2/3/4, an additional static GPS station about 19 km from the GPS buoy was placed to analyze how the accuracy of the measurements were influenced by the baseline length (see the top-left figure in Fig. 2). The static GPS station and the GPS buoy both had a reception frequency of 1 Hz.

The RBRsolo D tide loggers (Fig. 3b) were used as a TG to measure the sea/air pressure and obtain the relative sea level change. This kind of logger is compact, lightweight, and versatile, and can operate at depths of up to 20 m. It can collect accurate pressure and take the average pressure readings over long periods of time at frequencies up to 16 Hz. Two loggers were placed in each campaign. One was fixed to a stainless-steel pipe and measured the sea pressure at a frequency of 1 Hz. The other one was placed for measuring the air pressure, so that the actual sea pressure could be corrected against the air pressure. Both tide

Fig. 1. GPS buoy deployment in the ZW2 campaign. The buoy was moored near the wharf of Zhiwan Island. The TG and the static GPS station were placed on the island.

Table 1. The detailed information of the twelve campaigns

	ID	Date	Location	Static GPS station		Time length/h	Baseline/km
				Antenna	Receiver		
1	QLAN	August 5, 2014	Qinglan	Trimble 59900	Trimble Net R9	18.28	<1
2	DG1	May 2, 2015	Dangan Island	Trimble 59900	Trimble Net R9	5.69	<1
3	DJ	November 8, 2017	Dongji Island	South Net S9	South CR3-G3	2.01	<1
4	ZW1	March 18, 2018	Zhiwan Island	South Net S9	South CR3-G3	16.60	<1, 19
5	WLD1	December 16, 2019	Wailingding Island	South Net S9	South CR3-G3	16.71	<1, 19
6	ZW2	December 17, 2019	Zhiwan Island	South Net S9	South CR3-G3	3.03	<1, 19
7	ZW3	November 29, 2020	Zhiwan Island	South Net S9	South CR3-G3	2.33	<1, 19
8	SY	June 20, 2021	Sanya	South Net S9	South CR3-G3	6.00	<1
9	YGH	July 12, 2021	Yinggehai	Trimble 59900	Trimble Net R9	5.40	<1
10	ZW4	September 5, 2021	Zhiwan Island	South Net S9	South CR3-G3	3.50	<1, 19
11	DG2	September 6, 2021	Dangan Island	South Net S9	South CR3-G3	10.00	19
12	WLD2	September 7, 2021	Wailingding Island	South Net S9	South CR3-G3	18.00	<1, 19

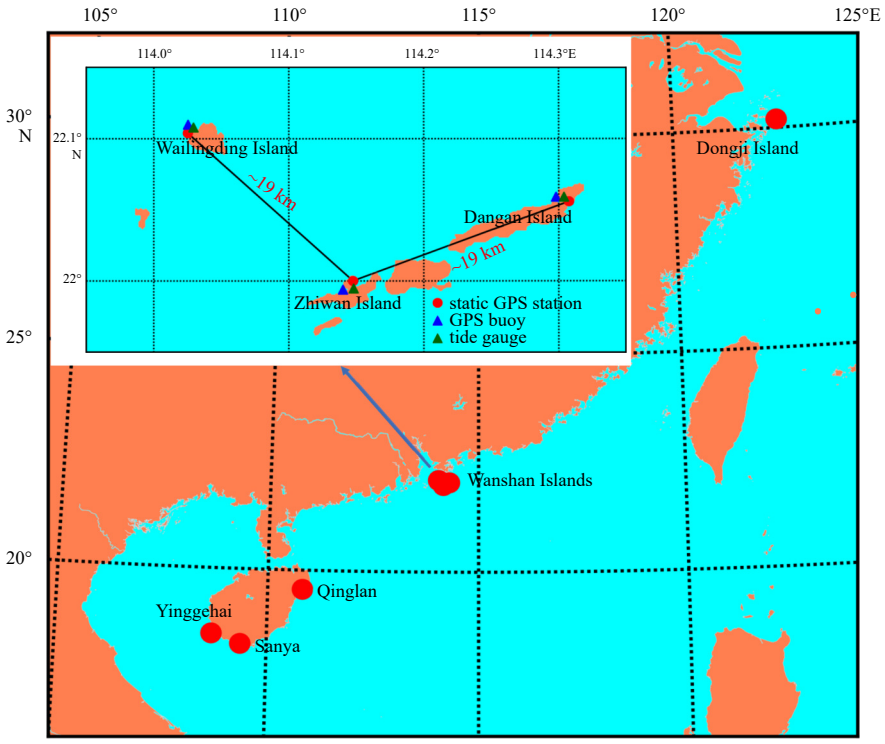

Fig. 2. Twelve campaigns conducted from 2014 to 2021. Campaigns 2, 4–7, 10–12 in Table 1 are shown in the top-left figure. In Campaigns 1–3 and 8–9, only one static GPS station was placed with a distance of <1 km between them. In Campaigns 4–7, 10 and 12, two static GPS stations were placed on Wailingding and Zhiwan islands, with a distance of about 19 km between them. In Campaign 11 (DG2), only one static GPS station was placed with a distance of about 19 km between them.

loggers were installed at less than 0.5 km from the GPS buoy in each campaign (Fig. 3). The temperature and salinity of sea water were measured by a CTD probe (SZC15-2 CTD). The real tide was calculated as described by Tang et al. (2008) and was then filtered through a 2-min lowpass filter, which were equal to the reciprocal of the span (Watson, 2005).

2.2 *GPS buoy solutions*

The quality of the GPS data was firstly checked using TEQC software. This is a powerful GNSS data pre-processing software developed by the UNAVCO Facility, its main features include format conversion, editing and quality checklist (Estey and Meertens, 1999). It can discover data problems, format conversion, edit and quality checklist, check the GNSS data quality, ionospheric delay, multi-path effects (MP1/2), the receiver cycle slips (o/slps), satellite signal to noise ratio (SNR, including SN1/2 and o/slps) and other information, so this software is widely used in GPS data pre-processing. The MP1/2 and SNR of the data were shown in Table 2. The satellite elevation cut-off was set to 10°, to eliminate the influence of the signals reflected by the ocean. All the MP1/2 results from each campaign were lower than 50 cm, and meet the quality need of the accurate GNSS measurement (Zuo et al., 2009; Jia et al., 2014; Wang et al., 2018).

The static GPS data was processed using GAMIT/GLOBK software (version 10.70). The choice of observation was the ionosphere-free linear combination (LC_AUTCLN) (Herring et al., 2018). The International Earth Rotation Service 2010 (IERS2010) solid Earth tide model and pole tide model and the FES2014

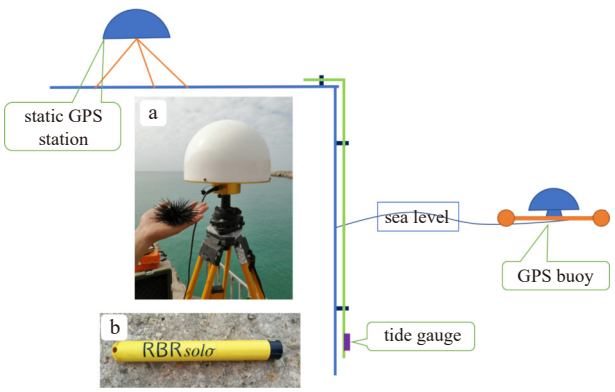

Fig. 3. Diagram of the static GPS station (a), tide gauge (TG) (b) and GPS buoy. The TG was fixed onto a stainless-steel tube that attached to the wharf to ensure its perpendicular. The GPS buoy was moored near the wharf and was less than 0.5 km from the TG.

Table 2. The quality of the GPS buoy data

Campaign ID	MP1/m	MP2/m	SN1	SN2	o/slps
QLAN	0.34	0.33	44.44	37.10	3 722
DG1	0.25	0.22	45.39	33.57	18 857
DJ	0.24	0.22	46.09	39.05	9 170
ZW1	0.23	0.22	45.29	34.13	38 426
WLD1	0.30	0.25	44.05	33.00	36 051
ZW2	0.28	0.23	43.74	31.97	19 644
ZW3	0.29	0.23	43.20	38.55	7 975
SY	0.36	0.28	42.58	38.60	4 395
YGH	0.27	0.22	42.95	37.36	7 954
ZW4	0.36	0.32	43.25	39.25	1 294
DG2	0.33	0.27	42.96	39.18	1 563
WLD2	0.26	0.26	43.40	39.41	3 989

ocean tide model were used for data processing (Li et al., 2020). We also employ International GNSS Service (IGS) precise orbits and absolute antenna phase center calibrations during the daily data processing. The daily solution of the static GPS stations in the campaigns was combined with at least 31 nearby distributed IGS stations collected from Scripps Orbit and Permanent Array Center (SOPAC) (Fig. 2). After the baseline computation using the GAMIT software, a whole-network adjustment was performed using GLOBK software where the coordinates and velocities of ITRF2014 core stations were used as the benchmarks (Jin et al., 2019). This will set an absolute datum of millimeter level for GPS buoy data solutions (Zhai et al., 2021).

Using the accurate coordinates of the static GPS stations from GAMIT/GLOBK, the kinematic solution of the GPS buoy was processed by TRACK module, which is a dynamic positioning module in GAMIT/GLOBK (Herring, 2012). The kinematic results comprised the XYZ, BLH coordinates and the integrated weighted RMS of the GPS buoy. TRACK uses the difference in the carrier phase observation value when processing the kinematic relative positioning and the phase difference is mainly used to solve the ambiguity of the whole cycle. This gave us the coordinates of the GPS buoy in the WGS84 ellipsoid. The continuous H element of the BLH represents the SSH after subtracting the height of the GPS antenna reference point above the waterline.

To evaluate the accuracy of the buoy, the data were processed using the TRACK module applying the Ultra-Rapid (IGU), Rapid (IGR), and Final (IGS) ephemeris, respectively. The buoy observations were also processed using the static GPS stations placed at a baseline length of 19 km. The SSH results were filtered with a moving average of 2 min to eliminate the ocean noise such as waves. These results were then compared with the data from the nearest TG. In the baseline length of 19 km, the satellite altimeters can avoid contaminating by the land, which distorts the waveforms (Cancet et al., 2013). Moreover, the CSRS-PPP tool was also used to derive the SSH and then compared with the TRACK solutions.

The dedicated GPS buoy was used for Cal/Val of SSH and significant wave height (SWH) of HY-2B/C altimeters for the in-orbit test. Such campaigns have been done in the Wanshan altimeter calibration site, which was built and operated by the National Satellite Ocean Application Service (NSOAS) (Chen et al., 2021; Zhai et al., 2022). The altimeter data was also achieved from the NSOAS (https://osdds.nsoas.org.cn/). Details of altimeter processing methods can be found in Chen et al. (2021).

3 Accuracy of GPS buoy

3.1 *The influence of different GPS ephemeris*

The SSH of the GPS buoy was obtained by processing with GAMIT/GLOBK and TRACK, using the IGU, IGR, and IGS products. All the height elements of the results were filtered by a weighted moving average with a time length of 2 min. The SSH estimates of the filtered time series were then extracted at times that were concurrent to the TG samples. The SSH estimates from the GPS buoy agreed relatively well with the TG data and had a standard deviation of less than 14 mm (Table 3). The results were generally consistent with those from Watson (2005) and Liu et al. (2014). The difference in the standard deviation of the three different ephemerides was less than 1 mm (Table 3).

Analysis of the GPS ephemeris data showed that the IGU ephemeris may have suffered from a deficiency in a few satellites. For instance, the GPS satellite number of PN30 and PN08 were lost on August 4, 2014 and May 2, 2015. The results were best from the IGS final products with minimum standard deviation of all the campaigns. This product combines the weighted averages of about nine analysis centers that are made available on a weekly basis, by Thursday, with a delay of between 12 d and 18 d. The IGR products are available daily, with a delay of about 17 h after the end of the previous observation day (the update period is between 17 d and 41 h). The IGR and IGS products have equivalent accuracy with orbit error of about 25 mm and satellite clock RMS of about 75 ps (http://www.igs.org/products#GPS).

The SSH of the GPS buoy processed by the IGR and IGS had similarly accuracy (Table 4), which mainly depends on its almost equivalent accuracy with the GPS final ephemeris. Unlike the IGU products, the IGR data do not lack GPS satellite data. Therefore, the rapid products (IGR) can be used to process the GPS data instead of the final products (IGS). The results from testing the altimeter calibration showed that the IGR product gave rapid solutions for the GPS buoy data. We can determine whether the results of the campaign are good from the quasi-time SSH of the GPS buoy.

3.2 *Comparisons with TGs*

The accuracy of the SSH of the buoy was obtained by comparing with the TG data in twelve campaigns. The 2 min filter was used to eliminate the influence of the variability of the ocean. There was no significant difference between the TG and the GPS buoy data when the baseline length was <1 km with a standard

Table 3. The GPS buoy data processed by different ephemeris (attributes in the following table) and the data from tide gauge (TG) of the twelve campaigns (unit: mm)

Campaign ID	Standard deviation			Max			Min		
	igs	*igr*	*igu*	*igs*	*igr*	*igu*	*igs*	*igr*	*igu*
QLAN	12.16	12.16	12.16	40.32	40.33	40.32	–47.09	–47.09	–47.09
DG1	13.58	13.59	13.60	61.04	61.01	61.02	–69.81	–69.83	–69.83
DJ	12.79	12.80	13.58	40.12	40.37	40.37	–25.88	–25.9	–25.96
ZW1	12.38	12.38	12.38	47.5	47.5	47.5	–69.61	–69.61	–69.61
WLD1	13.70	13.71	13.70	44.80	44.80	44.96	–51.11	–51.23	–51.23
ZW2	11.93	11.93	11.93	28.84	28.84	28.84	–39.30	–39.30	–39.30
ZW3	8.78	8.79	8.81	25.17	25.17	25.24	–23.89	–23.89	–23.89
SY	13.44	13.44	13.45	36.99	36.99	36.99	–36.37	–36.38	–36.37
YGH	10.42	10.39	10.41	25.13	25.14	25.13	–27.01	–27.01	–27.02
ZW4	8.73	8.73	8.75	37.76	37.76	37.80	–26.78	–26.78	–26.82
DG2	22.10	22.25	22.43	60.82	60.85	60.92	–49.73	–49.73	–49.85
WLD2	9.56	9.56	9.60	46.02	46.02	46.10	–32.59	–32.60	–32.65

Note: *igs*, *igr*, *igu*: the GPS buoy data achieved from the IGS, IGR and IGU products minus the TG data.

Table 4. GPS buoy solution of 19 km baseline length versus <1 km and the tide gauge (TG) data. There is only the standard bias (Std) for the comparison of 19 km baseline length solution vs. the TG data (unit: mm)

Campaign ID	Baseline length of about 19 km vs. <1 km		Baseline length of about 19 km vs. the TG data
	Std	bias	Std
ZW1	17.69	3.16	17.25
WLD1	23.54	24.76	28.20
ZW2	15.51	–31.10	21.40
ZW3	8.15	–1.38	13.84
ZW4	13.02	4.27	15.59
DG2	–	–	24.22
WLD2	25.22	24.76	25.03

bias of less than 14 mm after filtering (Fig. 4), because the static GPS station was very close to the GPS buoy, and the ionospheric and tropospheric conditions were similar (Herring, 2012).

However, in the ZW1 and SY campaigns, the SSH jumped and lost suddenly over a period of time (Fig. 5). This may be caused by weak GPS satellite coverage (Liu et al., 2014), multipath, or changes in the floating position of the buoy. This can serve as an indicator of cycle slip, which means a sudden jump that occurs when a carrier tracking loop misses a whole number of wavelengths in carrier phase measurements (Zhai et al., 2021). If the carrier cycle slip occurred, the coordinates become erroneous. As the TRACK solution of the position of this epoch is based on the information of the previous epoch or the initially input coordinates. It takes some time for the GPS receiver to resettle and gener-

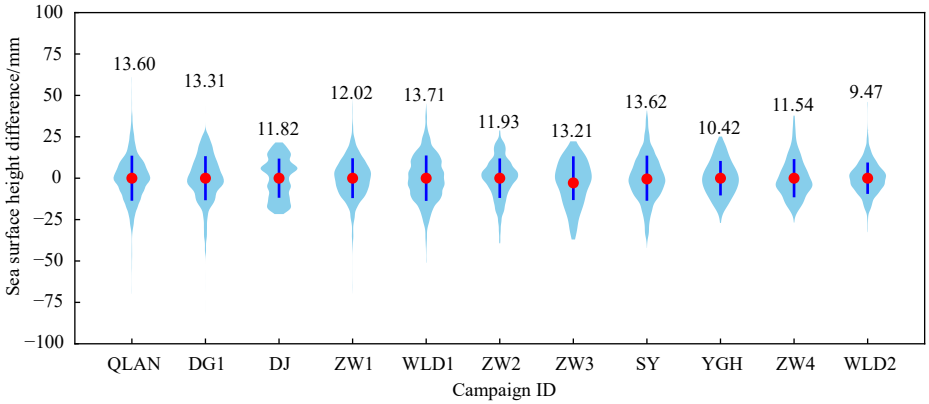

Fig. 4. Comparison of the buoy data and the tide gauge data. The blue lines are the standard bias of the comparison, which is also shown on the top of the violin (unit: mm).

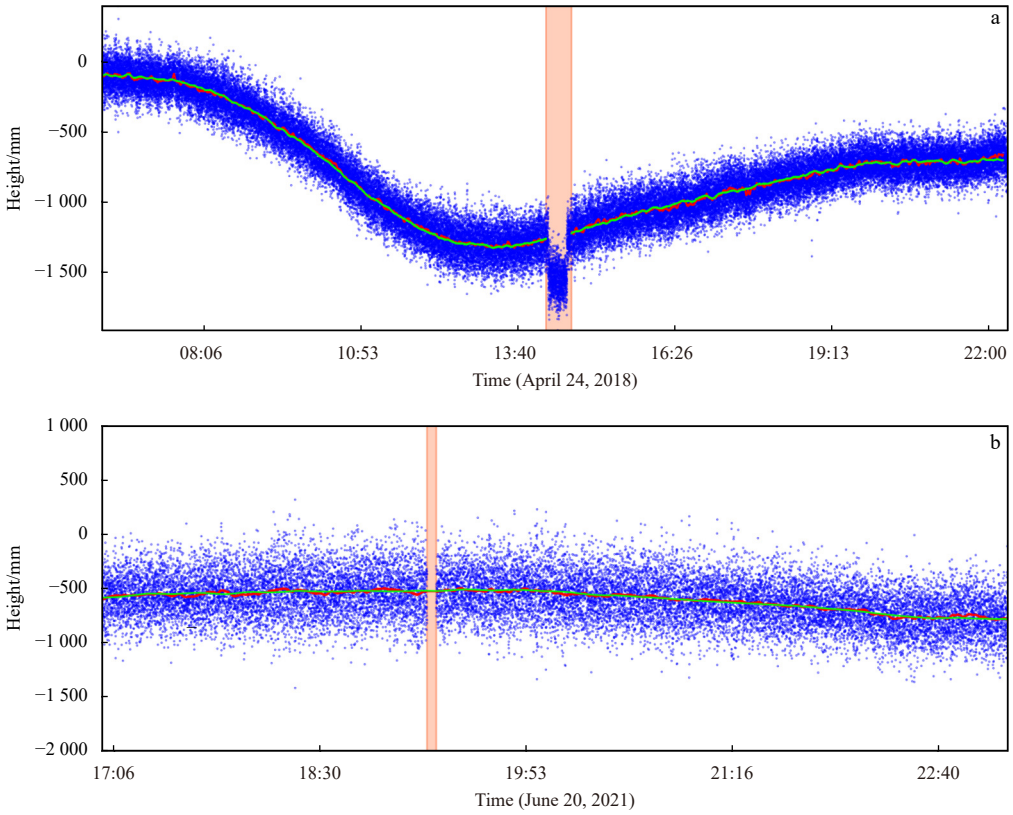

Fig. 5. Comparison of the ZW1 (a) and SY (b) buoy solution and the tide gauge (TG). The blue dots are the sea surface height (SSH) derived from the raw GPS buoy solutions. The red lines are the SSH filtered by the raw solutions, and the green lines are the TG data. The filled lightsalmon area represents the error or blank data of the measurements.

ate a re-convergence result when sudden jumps occurred like this. When it is in a relatively fixed position (usually with a moving range within 200 m) and the baseline length is less than 2 km, kinematic solutions can vanish quickly (Watson, 2005; Watson et al., 2008; Zhai et al., 2021). This takes only 15 min and 3 min to resettle in the ZW1 and SY campaigns when sudden jumps occurred, respectively.

3.3 *The influence of distance*

We wanted to determine how the baseline length affected the accuracy of the SSH results derived from the GPS buoy. The buoy was placed in a relatively specific position and the static GPS stations were placed 19 km from the buoy in the WLD2, DG2 and ZW1/2/3/4 campaigns (Table 1). The GPS buoy data were calculated for the two baseline lengths, i.e., <1 km and 19 km. The accuracy was evaluated by comparing the SSH with the TGs (Fig. 6 and Table 4).

There was good agreement between the SSH derived from the GPS buoy and the TGs with a standard bias of less than 26 mm (blue violin in Fig. 6). The GPS buoy solution of 19 km baseline length were also compared with the results of <1 km baseline length (red violin in Fig. 6). The bias between them varies between –31.10 mm and 24.79 mm, with a standard bias of 8.15–25.22 mm. This was because for short baselines (<2 km), the atmospheric delay of the static GPS station was similar with the GPS buoy kinematic station. Positioning can use L1 and L2 separately (less random noise). For longer baselines (>3 km), it uses the Melbourne-Wubena Wide Lane (MW-WL) to resolve L1–L2. Then a combination of techniques was used to determine L1 and L2 cycles separately. This can obtain the three-dimensional coordinates and unit weight mean square error of stations by single epoch in a given coordinate system (Herring, 2012). All these results showed high accuracy for SSH measurements. The results demonstrated that the SSH measurements of the GPS buoy has higher accuracy than the altimeters, and could be used to accomplish the Cal/Val of altimeters.

However, there are relatively large differences in ZW1 and WLD2 campaigns (Fig. 7). When the baseline length is <1 km, it takes 15 min to obtain a re-convergence result in the ZW1 campaigns. When the baseline length is 19 km, it takes 22 min, respectively. For the WLD2 campaign, the SSH derived from the GPS buoy showed good agreement with the TG with baseline length <1 km. However, the data has large differences in two clinic times with 19 km baseline length, and takes 38 min and 20 min to get a re-convergence result (filled orange area in Fig. 7). This may be caused by the following reasons. Firstly, there is either weak GPS satellite coverage, multipath, or changes in the flotation position of the buoy (Liu et al., 2014). Secondly, to process the data in TRACK, the numbers of GPS satellite signals received from the buoy and the static GPS stations need to be the same (Herring, 2012). At <1 km, more of the GPS signals are the same and the ionospheric and tropospheric conditions are more similar than at the 19 km baseline length, so the results at 1 km are less ambiguous and the atmospheric delay is more accurate. Irregular results are generally removed in data processing (Watson, 2005; Watson et al., 2008).

3.4 *Accuracy of the PPP technology*

The SSH of the GPS buoy data was derived using the CSRS-PPP tool operated by the Natural Resources Canada's Canadian Geodetic Survey (CGS). The CSRS-PPP is an online application for post-processing GNSS data that allows users to compute high accuracy positions from their raw observation data (Dawidowicz and Krzan, 2014). The CSRS-PPP uses precise GNSS satellite orbit ephemerides to recover enhanced positioning precisions in the International Terrestrial Reference Frame (ITRF), similar to GAMIT/GLOBK and TRACK.

The height element of the CSRS-PPP tool was filtered by a weighted moving average of 2 min which was the same with TRACK solutions. The differences between the PPP and TRACK results from the twelve campaigns are presented in Table 5 and Fig. 7. The bias from the GPS buoy solutions and the TRACK results varied between –132.0 mm and 165.5 mm and the standard deviations ranged from 17.4 mm to 56.0 mm (Fig. 8). In most cases, there were decimeter-level differences between the PPP heights and the TRACK heights. This meant that the SSH derived from the CSRS-PPP tool was not stable or accurate for calibration of satellite altimeters which had an accuracy of ~30 mm in SSH measurements (Ocean Surface Topography Mission, 2017).

4 Cal/Val of HY-2B/C altimeters

The GPS buoy was used for Cal/Val of HY-2 satellite altimeters. For HY-2A, the Cal/Val work had been done during 2013–2016 at many locations of China sea area (Zhai et al., 2019; Chen et al., 2019; Jiang et al., 2019). Here, the GPS buoy was used to accomplish the Cal/Val of SSH and SWH of HY-2B/C altimeters at the start of the satellite projects for the in-orbit test. The time ranged from October to December 2018 and November to

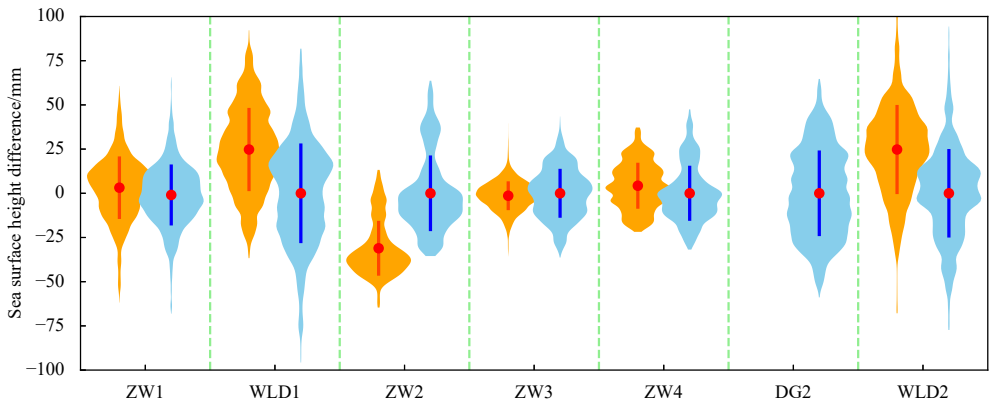

Fig. 6. Comparison of the GPS buoy results. The sky-blue violins represent the comparisons with the GPS buoy solution of <1 km baseline; the orange violins represent the comparisons with the tide gauges (TGs). The red dots are the bias, and the blue lines are the standard bias. There is comparison between the GPS buoy solution with a baseline length of 19 km and TG on DG2 campaign.

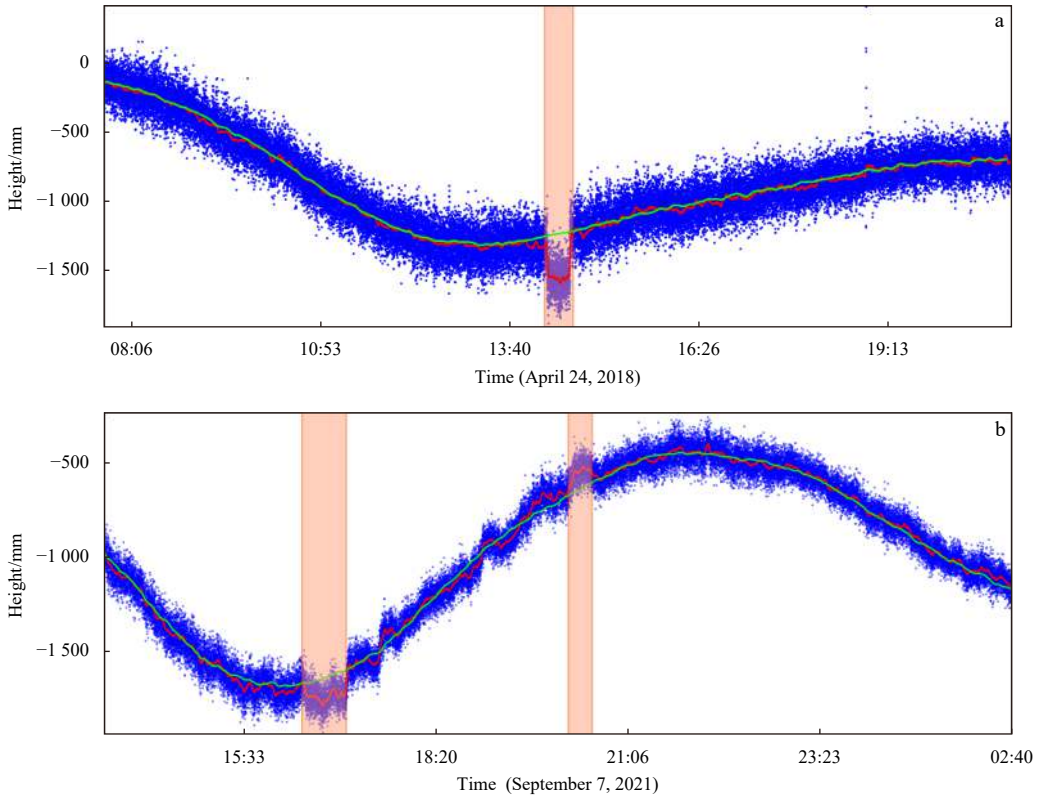

Fig. 7. Data of the ZW1 (a) and WLD2 (b) campaigns. Comparison of the buoy data and the tide gauge (TG) data. The blue dots are the sea surface height (SSH) derived from the raw GPS buoy solutions. The red lines are the SSH filtered by the raw solutions, and the green lines are the TG data. The filled lightsalmon area represents the irregular data of the measurements.

Table 5. The precise point positioning solutions minus the TRACK values (unit: mm)

Campaign ID	Mean	Std	Min	Max
QLAN	−81.8	29.8	−202.9	−04.3
DG1	−132.0	21.0	−190.2	−84.7
DJ	105.8	24.4	−21.8	154.6
ZW1	−29.1	39.6	−171.7	62.9
WLD1	71.2	20.5	−08.3	136.3
ZW2	12.1	56.0	−88.0	141.2
ZW3	165.5	17.4	100.6	222.0
SY	−9.9	19.5	−54.1	117.3
YGH	20.9	29.8	−16.5	75.1
ZW4	−10.2	24.4	−68.6	119.3
WLD2	0.3	30.6	−85.7	111.2

December 2020 for HY-2B and HY-2C, respectively (Fig. 9). A total of ten *in-situ* experiments have been conducted, with six for HY-2B and four for HY-2C.

The GPS buoy was moored at the location of the HY-2B altimeter footprints for six times at the Wanshan calibration site (WSCS) (Fig. 10a), three for Pass 375 and three for Pass 362. The baseline length between the static GPS station and the GPS buoy ranges from about 20 km to 40 km, accordingly. The estimated accuracy of the HY-2B altimeter's SSH has a 21.2 mm bias with a standard bias of 20.8 mm. Details of the calibration methods and results can be found in Chen et al. (2021). The SSH accuracy was 26 mm for a baseline length of about 20 km according to our research, and less than 35 mm for baseline length of 40 km (Zhai et al., 2019).

The HY-2C altimeter was also calibrated four times using the GPS buoy at WSCS, three for Pass 170 and one for Pass 185 (Fig. 10b). A static GPS station was placed on Zhiwan Island in the campaign. The GPS buoy was moored less than 0.5 km from the HY-2C footprints, and about 2 h before and after the altimeter overflights. The baseline length between the static GPS station and the GPS buoy was less than 20 km, which could measure the SSH in an accuracy of less than 35 mm according to Section 3.2. An example for HY-2C calibration using the GPS buoy was shown in Fig. 11. A system error or algorithm error was detected in the in-orbit calibration campaign of HY-2C, and this was corrected in the publicly available altimeter data. The standard bias of the Cal/Val results was 7.9 mm, which demonstrated high precision of altimeter measurements.

The GPS buoy was also used to measure the SWH, which was determined by the formula SWH = 4 $(\zeta^2)^{1/2}$, where $(\zeta^2)^{1/2}$ is the standard deviation of surface displacement (Stewart, 2008). Here, it was determined using the GPS buoy solutions (such as the blue dots in Figs 5 and 7) in every 30 min (Xu et al., 2016). The SWHs of the HY-2B/C altimeters were validated using the GPS buoy and Directional Wave-rider (DWR-MkIII, Fig. 12). The two equipments were towed at the end of the ship at the overflight of the altimeters. The validation results of the altimeter SWH minus GPS buoy were (5.63±6.07) cm and (−2.93±3.87) cm for HY-2B and HY-2C, respectively. The GPS buoy derived SWH shows good agreements with the DWR-MkIII.

5 Conclusions and discussion

From 2014 to 2021, twelve campaigns were conducted to evaluate the stability and accuracy of the dedicated GPS buoy. There were good agreements between the SSH measured by the GPS buoy and the TGs. When the baseline length was <1 km, the

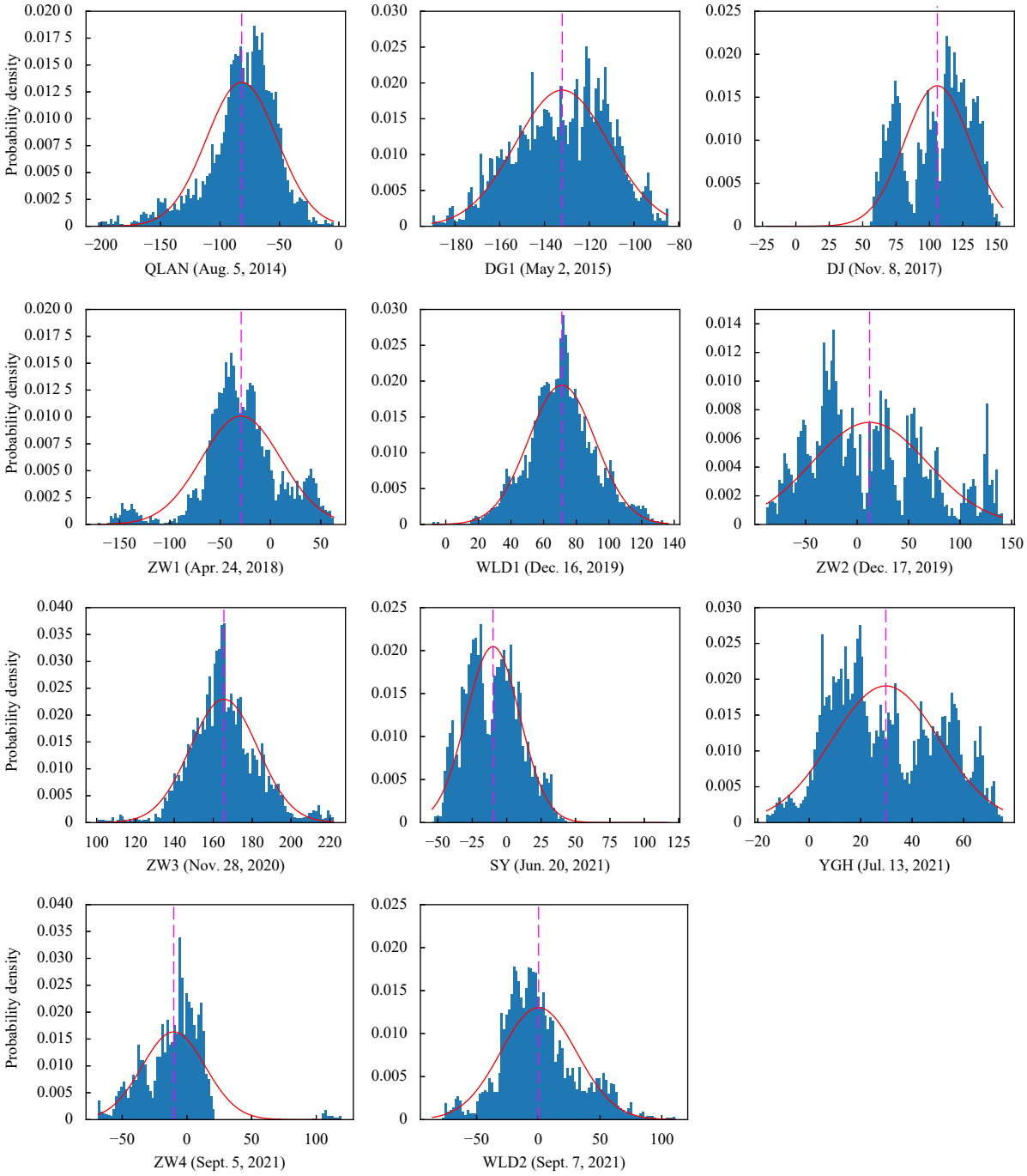

Fig. 8. Differences between precise point positioning (PPP) and TRACK results. The standard deviations were sometimes larger for the PPP results than for the TRACK results, as for the ZW2 campaigns. There was a deviation of more than 100 mm for the DG1, DJ and ZW3 campaign, but the results were closer for the ZW1, SY and YGH campaign. Units of the *x*-axis are mm.

standard deviation of the GPS buoy was less than 14 mm compared with the sea level measured by the TG, which showed that the SSH measurements from the buoy were precise and stable. However, there were a few sudden jumps in the buoy solution data, perhaps because of a weak GPS satellite coverage, multipath, or a change in the flotation position of the buoy. These data should be removed. The solutions obtained using the IGS, IGR, and IGU ephemeris were not significantly different. We found that the IGR or IGS ephemeris gave the best results. The baseline length can influence the accuracy of the SSH measurements. When the baseline length was 19 km, the accuracy was about 30 mm with a standard deviation of less than 26 mm. This is acceptable for Cal/Val of satellite altimeters. However, it took a longer time to obtain a re-convergence result for a station at 19 km than at 1 km if there were sudden jumps, because the solution depended on the time of matching the GPS satellite signals from the buoy with those from the static GPS stations. The SSH results obtained from the CSRS-PPP tool were relatively unstable with an accuracy of decimeters. This tool cannot meet the accuracy requirements of satellite altimeter calibrations.

The SSH and SWH of HY-2B/C altimeters were calibrated and validated using the GPS buoy and wave-rider, respectively. The

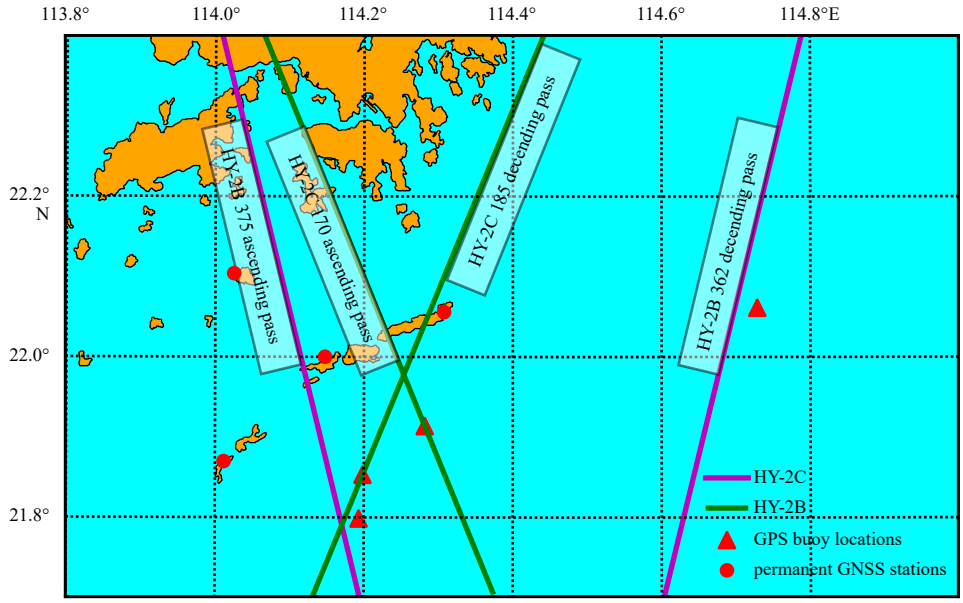

Fig. 9. GPS buoy placement in the Cal/Val of HY-2B/C altimeters. The red triangulars represent the location of the GPS buoy displacement. There are two or three GPS buoy displacements for altimeter calibrations in each point. The red dots represent the permanent GNSS stations in Wanshan calibration site. The distance of the GPS buoy was less than 0.5 km from the footprint of altimeters.

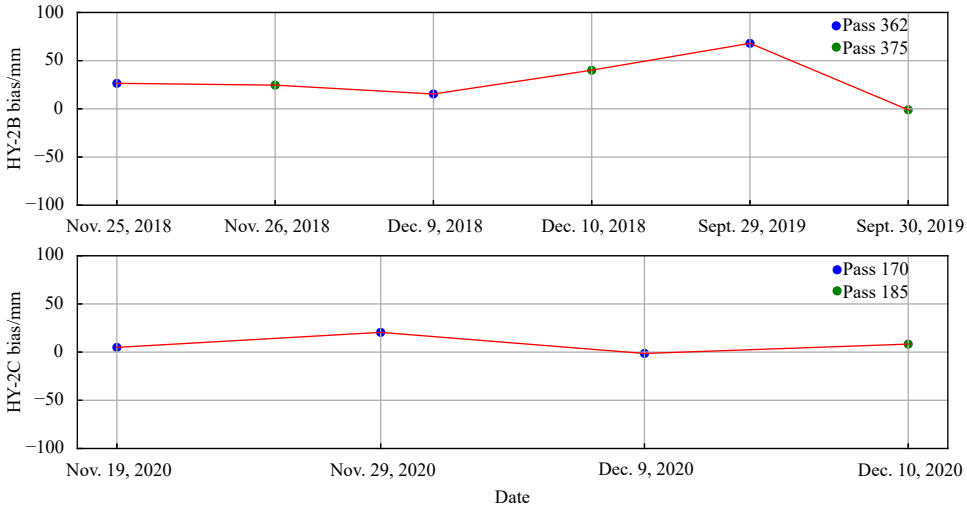

Fig. 10. Sea surface height calibration of the HY-2B/C altimeters using the dedicated GPS buoy.

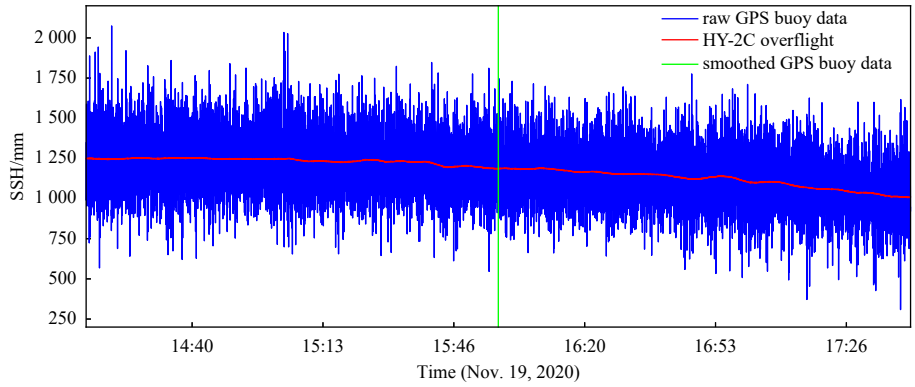

Fig. 11. An example of HY-2C calibration using the dedicated GPS buoy. The blue line represents the GPS buoy data processed using the GAMIT/GLOBK+TRACK; the green line represents the smoothed GPS buoy solution data; the lime line represents the time of HY-2C overflight.

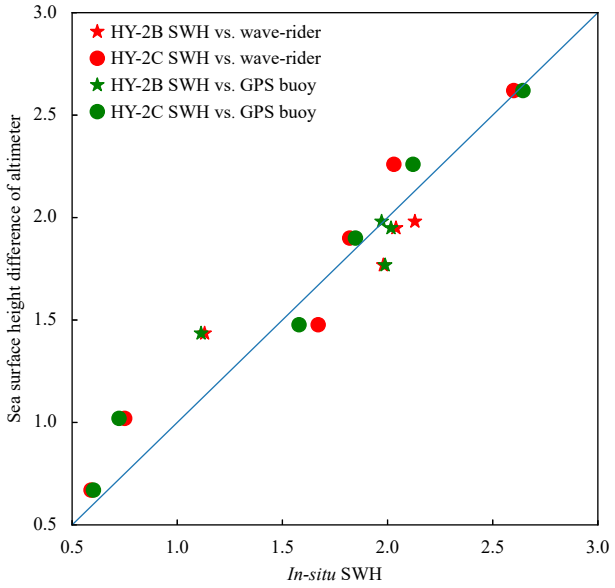

Fig. 12. Significant wave height (SWH) comparison between the altimeters, wave-rider and GPS buoy. The bias of the GPS buoy minus wave-rider was (–4.75±16.13) cm in the ten campaigns.

standard bias of SSH was 20.8 mm and 7.9 mm for HY-2B and HY-2C, respectively. The SWH derived from the GPS buoy shows good agreements with the DWR-MkIII and altimeters.

The twelve campaigns were carried out relatively close to the coast (about 1 km) in relatively calm sea conditions with a baseline length of up to 19 km. Altimeter calibrations are generally done in open sea areas, often under high sea conditions, with about 15–30 km between the static GPS station and the GPS buoy. More similar campaigns are required to evaluate the accuracy of the GPS buoy. The dedicated GPS buoy mentioned in this paper cannot be moored at a relatively static location for too long, as the lithium battery inside the buoy can only supply power for about 7 d. Therefore, a mooring GPS buoy was designed for operational applications of Cal/Val of the altimeters in a relatively fixed position which can be powered by solar energy and can work continuously for up to half a year (National Ocean Technology Center, 2020).

There are also other methods to derive the SSH of the buoy without the support of the static GPS stations, such as GINS developed by CNES (Crétaux et al., 2018), PRIDE PPP-AR developed by Wuhan University (Geng et al., 2019), Trimble-RTX technology (Chen et al., 2011) etc. Such tools or technology can be integrated into buoy or ship borne platform, and will provide the basic technical conditions for the calibration of the whole sea area altimeter or the three-dimensional imaging radar altimeter.

Acknowledgements

We thank a number of people for contributing to this study, including Xiaoxu Zhang, Qian Zhang, Hongguang Zhu, Debin Qin, Da Zhao, Liping Huang, the staff of the Qinglan Marine Environment Monitoring Station and the crews of the R/V *Runjiang 1* for their support in acquiring tidal level data, static GPS stations and buoy layout.

References

Ardalan A A, Jazireeyan I, Abdi N, et al. 2018. Evaluation of SARAL/AltiKa performance using GNSS/IMU equipped buoy in Sajafi, Imam Hassan and Kangan Ports. Advances in Space Research, 61(6): 1537–1545, doi: 10.1016/j.asr.2018.01.001

Babu K N, Shukla A K, Suchandra A B, et al. 2015. Absolute calibration of SARAL/AltiKa in Kavaratti during its initial calibration-validation phase. Marine Geodesy, 38(S1): 156–170, doi: 10.1080/01490419.2015.1045639

Bonnefond P, Exertier P, Laurain O, et al. 2013. GPS-based sea level measurements to help the characterization of land contamination in coastal areas. Advances in Space Research, 51(8): 1383–1399, doi: 10.1016/j.asr.2012.07.007

Cancet M, Bijac S, Chimot J, et al. 2013. Regional *in situ* validation of satellite altimeters: calibration and cross-calibration results at the Corsican sites. Advances in Space Research, 51(8): 1400–1417, doi: 10.1016/j.asr.2012.06.017

Chen Xiaoming, Allison T, Cao Wei, et al. 2011. Trimble RTX, an innovative new approach for network RTK. In: Proceedings of the 24th International Technical Meeting of the Satellite Division of the Institute of Navigation. Portland, OR: Oregon Convention center: 2214–2219

Chen Chuntao, Zhai Wanlin, Yan Longhao, et al. 2014. Assessment of the GPS buoy accuracy for altimeter sea surface height calibration. In: Proceedings of the 2014 IEEE Geoscience and Remote Sensing Symposium. Quebec City, Canada: IEEE, 3101–3104, doi: 10.1109/IGARSS.2014.6947133

Chen Chuntao, Zhu Jianhua, Ma Chaofei, et al. 2021. Preliminary calibration results of the HY-2B altimeter's SSH at China's Wanshan calibration site. Acta Oceanologica Sinica, 40(5): 129–140, doi: 10.1007/s13131-021-1745-y

Chen Chuntao, Zhu Jianhua, Zhai Wanlin, et al. 2019. Absolute calibration of HY-2A and Jason-2 altimeters for sea surface height using GPS buoy in Qinglan, China. Journal of Oceanology and Limnology, 37(5): 1533–1541, doi: 10.1007/s00343-019-8216-8

Crétaux J F, Bergé-Nguyen M, Calmant S, et al. 2018. Absolute calibration or validation of the altimeters on the Sentinel-3A and the Jason-3 over Lake Issykkul (Kyrgyzstan). Remote Sensing, 10(11): 1679, doi: 10.3390/rs10111679

Dawidowicz K, Krzan G. 2014. Coordinate estimation accuracy of static precise point positioning using on-line PPP service, a case study. Acta Geodaetica et Geophysica, 49(1): 37–55, doi: 10.1007/s40328-013-0038-0

Dong Xiaojun, Woodworth P, Moore P, et al. 2002. Absolute calibration of the TOPEX/POSEIDON altimeters using UK tide gauges, GPS, and precise, local geoid-differences. Marine Geodesy, 25(3): 189–204, doi: 10.1080/01490410290051527

Estey L H, Meertens C M. 1999. TEQC: The multi-purpose toolkit for GPS/GLONASS data. GPS Solutions, 3(1): 42–49, doi: 10.1007/pl00012778

Fu L L, Christensen E J, Yamarone C A Jr, et al. 1994. TOPEX/POSEIDON mission overview. Journal of Geophysical Research, 99(C12): 24369–24381, doi: 10.1029/94JC01761

Geng Jianghui, Chen Xingyu, Pan Yuanxin, et al. 2019. PRIDE PPP-AR: an open-source software for GPS PPP ambiguity resolution. GPS solutions, 23(4): 91

Herring T A. 2012. TRACK GPS Kinematic Positioning Program, Version 1.07. Cambridge, MA: Massachusetts Institute of Technology

Herring T A, King R W, Folyd M A, et al. 2018. Introduction to GAMIT/GLOBK Release 10.7. Massachusetts Institute of Technology. http://www-gpsg.mit.edu/gg/docs/Intro_GG.pdf[2018-06-07/2018-06-20]

Jia Zhige, Chen Zhengsong, Wang Dijin, et al. 2014. The quality test of TOPCON NET-G3A GNSS receiver. Applied Mechanics and Materials, 511–512: 290–293, doi: 10.4028/www.scientific.net/AMM.511-512.290

Jiang Xingwei, Jia Yongjun, Zhang Youguang. 2019. Measurement analyses and evaluations of sea-level heights using the HY-2A satellite's radar altimeter. Acta Oceanologica Sinica, 38(11): 134–139, doi: 10.1007/s13131-019-1503-6

Jin Honglin, Gao Yuan, Su Xiaoning, et al. 2019. Contemporary crustal tectonic movement in the southern Sichuan-Yunnan block based on dense GPS observation data. Earth and Planet-

ary Physics, 3(1): 53–61, doi: 10.26464/epp2019006
Kato T, Terada Y, Nagai T, et al. 2010. Tsunami monitoring system using GPS buoy—Present status and outlook. In: 2010 IEEE International Geoscience and Remote Sensing Symposium. Honolulu, HI, USA: IEEE, 3043–3046, doi: 10.1109/IGARSS.2010.5654449
Li Fei, Zhang Qingchuan, Zhang Shengkai, et al. 2020. Evaluation of spatio-temporal characteristics of different zenith tropospheric delay models in Antarctica. Radio Science, 55(5): e2019RS006909, doi: 10.1029/2019RS006909
Lin Yen-Pin, Huang Ching-Jer, Chen Sheng-Hsueh, et al. 2017. Development of a GNSS buoy for monitoring water surface elevations in estuaries and coastal areas. Sensors, 17(1): 172, doi: 10.3390/s17010172
Liu Yalong, Tang Junwu, Zhu Jianhua, et al. 2014. An improved method of absolute calibration to satellite altimeter: A case study in the Yellow Sea, China. Acta Oceanologica Sinica, 33(5): 103–112, doi: 10.1007/s13131-014-0476-8
Martinez-Benjamin J J, Martinez-Garcia M, Lopez S G, et al. 2004. Ibiza absolute calibration experiment: survey and preliminary results. Marine Geodesy, 27(3–4): 657–681, doi: 10.1080/01490410490883342
Ménard Y, Jeansou E, Vincent P. 1994. Calibration of the TOPEX/POSEIDON altimeters at Lampedusa: additional results at harvest. Journal of Geophysical Research: Oceans, 99(C12): 24487–24504, doi: 10.1029/94JC01300
Ocean Surface Topography Mission. 2017. Jason-3 Products Handbook. Issue: 1, Rev: 4. https://www.ospo.noaa.gov/Products/documents/hdbk_j3.pdf [2018-10-20/2019-08-17]
Salleh A M, Daud M E. 2015. Development of a GPS buoy for ocean surface monitoring: initial results. World Academy of Science, Engineering and Technology, 9(6): 769–772, doi: 10.5281/zenodo.1109493
Stewart R H. 2008. Introduction to Physical Oceanography. Texas: Texas A&M University
Tang Yuxiang, Sun Hongliang, Hu Xiaomin, et al. 2008. GB/T 12763.2-2007. Specifications for oceanographic survey-Part 2: Marine hydrographic observation (in Chinese). Beijing: Standards Press of China
Wang Nazi, Xu Tianhe, Gao Fan, et al. 2018. Sea level estimation based on GNSS dual-frequency carrier phase linear combinations and SNR. Remote Sensing, 10: 470, doi: 10.3390/rs10030470
Watson C S. 2005. Satellite altimeter calibration and validation using GPS buoy technology [dissertation]. Hobart: University of Tasmania
Watson C, Coleman R, Handsworth R. 2008. Coastal tide gauge calibration: A case study at Macquarie Island using GPS buoy techniques. Journal of Coastal Research, 2008(244): 1071–1079, doi: 10.2112/07-0844.1
Xu Xiyu, Xu Ke, Shen Hua, et al. 2016. Sea surface height and significant wave height calibration methodology by a GNSS buoy campaign for HY-2A altimeter. IEEE Journal of Selected Topics in Applied Earth Observations and Remote Sensing, 9(11): 5252–5261, doi: 10.1109/JSTARS.2016.2584626
Zhai Wanlin, Zhu Jianhua, Chen Chuntao, et al. 2019. Calibration of HY-2A satellite altimeter based on GPS bouy. In: Proceedings of the 2019 IEEE International Geoscience and Remote Sensing Symposium. Yokohama, Tokyo: IEEE, 8300–8303, doi: 10.1109/IGARSS.2019.8900272
Zhai Wanlin, Zhu Jianhua, Fan Xiaohui, et al. 2021. Preliminary calibration results for Jason-3 and Sentinel-3 altimeters in the Wanshan Islands. Journal of Oceanology and Limnology, 39(2): 458–471, doi: 10.1007/s00343-020-9251-1
Zhai Wanlin, Zhu Jianhua, Lin Mingsen, et al. 2022. GNSS data processing and validation of the altimeter zenith wet delay around the Wanshan Calibration Site. Remote Sensing, 14, 6235, doi: 10.3390/rs14246235
Zhou Boye, Watson C, Legresy B, et al. 2020. GNSS/INS-equipped buoys for altimetry validation: Lessons learnt and new directions from the Bass Strait validation facility. Remote Sensing, 12(18): 3001, doi: 10.3390/rs12183001
Zumberge J F, Heflin M B, Jefferson D C, et al. 1997. Precise point positioning for the efficient and robust analysis of GPS data from large networks. Journal of Geophysical Research: Solid Earth, 102(B3): 5005–5017, doi: 10.1029/96JB03860
Zuo Xianqing, Bu Jinwei, Li Xiangxin, et al. 2019. The quality analysis of GNSS satellite positioning data. Cluster Computing, 22(3): 6693–6708, doi: 10.1007/s10586-018-2524-1